[redacted]

Copy 17

NASA TM X-412

NASA TM X-412

TECHNICAL MEMORANDUM

X-412

REFERENCE

CORRELATION OF BOUNDARY-LAYER TRANSITION RESULTS ON HIGHLY COOLED BLUNT BODIES

By Richard J. Wisniewski

Lewis Research Center
Cleveland, Ohio

CLASSIFICATION CHANGED
To Unclassified
By authority of H G Maines
Date 10-1-71
prma

CLASSIFIED DOCUMENT - TITLE UNCLASSIFIED

This material contains information affecting the national defense of the United States within the meaning of the espionage laws, Title 18, U.S.C., Secs. 793 and 794, the transmission or revelation of which in any manner to an unauthorized person is prohibited by law.

NATIONAL AERONAUTICS AND SPACE ADMINISTRATION

WASHINGTON October 1960

[redacted]

D[redacted]

NATIONAL AERONAUTICS AND SPACE ADMINISTRATION

TECHNICAL MEMORANDUM X-412

CORRELATION OF BOUNDARY-LAYER TRANSITION RESULTS ON HIGHLY COOLED BLUNT BODIES*

By Richard J. Wisniewski

SUMMARY

Boundary-layer transition data on two types of highly cooled blunt bodies are correlated in terms of the ratio of wall to total enthalpy and the Reynolds number based on displacement thickness. The proposed correlation indicates that cooling may cause the boundary layer to go from laminar to turbulent flow.

INTRODUCTION

In recent years a large amount of transition data has been obtained on blunt shapes because of the numerous experimental programs initiated to determine the conditions under which transition will occur during reentry. Correlations of these results were attempted in the investigation of references 1 to 3. None of these correlations are wholly successful or satisfying.

The purpose of this report is to present a new correlation of the aforementioned data by revising the correlation first presented in reference 3. The correlation of reference 3 is based on the ratio of wall to total enthalpy and the ratio of the local-displacement-thickness Reynolds number to the local Mach number. Although this parameter correlates the data well, it is not based on a physical model, nor is the displacement thickness calculated using real-gas boundary-layer solutions. In the present correlation[1], real-gas boundary-layer solutions provided by AVCO are used to calculate the displacement thickness. Many of the consequences and implications of this new correlation are not fully understood.

---

[1] This revised correlation was first presented at the 1960 Bumblebee Aerodynamics Conference, May 9-10 at Ann Arbor, Michigan.

---

*Title, Unclassified. D[redacted]

SYMBOLS

a	speed of sound
d	body diameter
f_η	defined by eq. (A14)
g	defined by eq. (A14)
H	total stream enthalpy
H^*	form factor, δ^*/θ
H^*_{TR}	transformed form factor, $\delta^*_{TR}/\theta_{TR}$
M	Mach number
$Re_{d,1}$	free-stream Reynolds number based on body diameter, $\rho_1 u_1 d/\mu_1$
Re_{δ^*}	displacement-thickness Reynolds number, $\rho_e u_e \delta^*/\mu_e$
Re_θ	momentum-thickness Reynolds number, $\rho_e u_e \theta/\mu_e$
r	axial radius
S	defined by eq. (A14)
u	velocity
x	distance along body surface
y	distance normal to body surface
β	pressure-gradient parameter
δ^*	displacement thickness
η	defined by eq. (A14)
θ	momentum thickness
μ	absolute viscosity
ξ	defined by eq. (2)
ρ	density
φ	angle between normal to body surface and free-stream direction

Subscripts:

e local free-stream conditions at edge of boundary layer

TR transformed coordinate system

t transition conditions

w conditions at wall

0 stagnation conditions behind normal shock

1 free-stream conditions ahead of shock

Superscripts:

— transformed plane

REDUCTION OF DATA

Location of Transition

The present report uses data obtained on hemispheres and a large blunt cone. Table I lists all the data used in this report as well as the various references from which the transition locations were obtained. No data from roughened bodies are included. The reasons for the exclusion of these transition data are presented in the text.

Displacement-Thickness Reynolds Number

In addition to the quantities obtained from the various references listed in table I, the Reynolds number based on displacement thickness is needed. This can be obtained from the momentum-thickness Reynolds number and the form factor as follows:

$$Re_{\delta^*} = H^* Re_\theta \tag{1}$$

where

$$H^* = \delta^*/\theta$$

$$Re_\theta = \rho_e u_e \theta/\mu_e$$

Calculation of Re_θ is made with the assumption of isentropic flow at the edge of the boundary layer from the stagnation point to the point of interest. The flow properties are then calculated using an effective specific-heat ratio, which approximates real-gas effects. This effective specific-heat ratio is varied as suggested in reference 2. The calculations of the momentum thickness are based on the methods outlined in reference 4. Thus, the momentum-thickness Reynolds number including real-gas effects is expressed as

$$Re_\theta = \frac{\Delta\sqrt{2\xi}}{\mu_e r}\left[0.491(1 - 0.090\ \beta^{0.4})\left(\frac{\rho_0\mu_0}{\rho_w\mu_w}\right)^{0.386}\right] \tag{2}$$

where

$$\xi = \int_0^x \rho_w\mu_w u_e r^2\ dx$$

$$\beta = \frac{2d\ \ln\ u_e}{d\ \ln\ \xi}$$

The pressure-gradient parameter β has a value of 1/2 at the stagnation point and around a hemisphere can be approximated as

$$\beta = \frac{2\displaystyle\int_0^\varphi \varphi\ \cos^2\varphi\ \sin^2\varphi\ d\varphi}{\varphi^2\ \cos^2\varphi\ \sin^2\varphi} \tag{3}$$

Although equation (3) is based on the assumptions of a perfect gas and Newtonian flow, it is reasonably accurate for real-gas flows for angular positions up to 60°.

Once Re_θ is obtained, all that is required for the calculation of Re_{δ^*} is the form factor. An approximate method for obtaining a form factor which includes real-gas effects is given in the appendix.

RESULTS AND DISCUSSION

Correlation of Hemisphere Data

Since different causes (e.g., surface roughness, cooling) have been postulated for the initiation of transition on cooled hemispheres, several correlations have been attempted to determine what parameters strongly influence transition on cooled hemispheres. An empirical correlation parameter which is independent of roughness is considered in reference 3. This correlation is based on the ratio of wall to total enthalpy H_w/H_0 and the ratio of the local displacement-thickness Reynolds number to the local Mach number Re_{δ^*}/M_e. Although this parameter correlates the data well, it is not based on a physical model, nor is the displacement thickness calculated using real-gas boundary-layer solutions.

Presented in figure 1 are the hemisphere data of table I in terms of the ratio of wall to total enthalpy and the local-displacement-thickness Reynolds number based on real-gas properties and real-gas boundary-layer solutions. For values of the ratio of wall to total enthalpy greater than 0.15, the data are well correlated, and a region between laminar and turbulent flow is clearly defined. It is also interesting to note in figure 1 that, at constant values of displacement-thickness Reynolds number, cooling causes the boundary layer to go from laminar to turbulent flow. The premature transition found here with cooling is contrary to the trends predicted by small-disturbance theory.

However, at values of the enthalpy ratio less than 0.15, the shock-tube results of reference 4 and the flight results of reference 1 show some disagreement. It is not known whether this disagreement is due to scatter in the flight data or some type of shock-tube effect.

Transition as Affected by Roughness

It is evident from available literature that surface roughness will affect the transition results. However, since it is clearly shown in reference 5 that not only the height but the type of the roughness is important, the only legitimate analysis that can be undertaken is on surfaces of the same type of roughness. Since the types of roughness on the hemispheres compared are quite different, no attempt is made to analyze the effect of surface roughness on transition data.

Extension of Correlation to Other Shapes

Since many practical blunt-nose shapes are not hemispherical, it is desirable to show that the correlation of transition data from other shapes can be attained. A plot of transition data on a large blunt cone is shown in figure 2. This figure also shows good correlation.

CONCLUDING REMARKS

A reasonable correlation of transition results on a hemisphere and a large blunt cone has been attained. The correlation indicates that cooling may cause the boundary layer to go from laminar to turbulent flow.

Since the present correlation as well as the data contradict the trend with cooling predicted by small-disturbance theory, additional theoretical and experimental studies are required. Detailed investigations which attempt to determine the origin of the flow disturbances have been initiated in reference 6. Studies such as this should be encouraged, since they will eventually lead to a basic understanding of the transition problem. A weakness in the present correlation is the fact that it is not motivated by any physical model. More basic studies are required if the usefulness of the present correlation is ever to be determined.

Lewis Research Center
National Aeronautics and Space Administration
Cleveland, Ohio, August 15, 1960

APPENDIX - FORM FACTOR

The form factor is defined as

$$H^* \equiv \delta^*/\theta \tag{A1}$$

where

$$\delta^* \equiv \int_0^\infty \left(1 - \frac{\rho u}{\rho_e u_e}\right) dy \tag{A2}$$

$$\theta \equiv \int_0^\infty \left(1 - \frac{u}{u_e}\right) \frac{\rho u}{\rho_e u_e}\, dy \tag{A3}$$

The density distribution is now approximated as

$$\frac{\rho_e}{\rho} \approx \frac{\rho_e}{\rho_w}\frac{H}{H_w} - \left(\frac{\rho_e H_e}{\rho_w H_w} - 1\right)\left(\frac{u}{u_e}\right)^2 \tag{A4}$$

This relation is used in reference 7, and, since it matches both at the wall and at the edge of the boundary layer, it is within the accuracy needed for the present calculation. Equations (A4) and (A2) may be combined to yield

$$\delta^* \approx -\int_0^\infty \left(1 - \frac{u}{u_e}\right)\frac{\rho u}{\rho_e u_e}\, dy + \frac{\rho_e H_e}{\rho_w H_w}\int_0^\infty \left(1 - \frac{u}{u_e}\right)\frac{\rho u}{\rho_e u_e}\, dy + \frac{\rho_e H_e}{\rho_w H_w}\int_0^\infty \left(\frac{H}{H_e} - \frac{u}{u_e}\right)\frac{\rho}{\rho_e}\, dy \tag{A5}$$

As in reference 7, the following are defined:

$$\theta_{TR} = \int_0^\infty \left(1 - \frac{\bar{u}}{\bar{u}_e}\right)\frac{\bar{u}}{\bar{u}_e}\, d\bar{y} \tag{A6}$$

$$\delta^*_{TR} = \int_0^\infty \left(1 - \frac{\bar{u}}{\bar{u}_e} - S\right) d\bar{y} \tag{A7}$$

where

$$
\left.
\begin{aligned}
\bar{u} &= u/a \\
\bar{y} &= a\int\rho\ dy \\
S &= 1 - H/H_e
\end{aligned}
\right\}
\qquad \text{(A9)}
$$

The barred quantities represent quantities in a transformed coordinate system. Equations (A6) and (A7) in terms of the physical coordinate system become

$$
\theta_{TR} = a\rho_e \int_0^\infty \left(1 - \frac{u}{u_e}\right) \frac{\rho u}{\rho_e u_e}\ dy
$$

or

$$
\theta_{TR} = a\rho_e\theta \qquad \text{(A10)}
$$

$$
\delta^*_{TR} = a\rho_e \int_0^\infty \left(\frac{H}{H_e} - \frac{u}{u_e}\right) \frac{\rho}{\rho_e}\ dy \qquad \text{(A11)}
$$

Substitution of equations (A10) and (A11) in equation (A5) yields

$$
\frac{\delta^*}{\theta} \equiv H^* \approx \left[-1 + \frac{\rho_e H_e}{\rho_w H_w}\left(1 + \frac{\delta^*_{TR}}{\theta_{TR}}\right)\right] \qquad \text{(A12)}
$$

where $\delta^*_{TR}/\theta_{TR}$ can be thought of as the transformed form factor H^*_{TR}.

In terms of the notation of reference 8 the transformed form factor becomes

$$
H^*_{TR} = \frac{\int_0^\infty (g - f_\eta)d\eta}{\int_0^\infty (1 - f_\eta)d\eta} \qquad \text{(A13)}
$$

where

$$
\left.
\begin{aligned}
f_\eta &= \frac{u}{u_e} = \frac{\bar{u}}{\bar{u}_e} \\
g &= \frac{H}{H_e} = 1 - S \\
\eta &= \frac{u_e r}{\sqrt{2\xi}} \frac{\bar{y}}{a}
\end{aligned}
\right\}
\qquad \text{(A14)}
$$

and ξ is defined by equation (2).

The integrals in equation (A13) were evaluated using the real-gas boundary-layer profiles. (These profiles were obtained in private correspondence from Dr. Kemp of AVCO and are the same profiles as used in ref. 8.) Values of $H_{TR} + 1$ are presented in figure 3 for various values of the pressure-gradient parameter β and the ratio $\rho_0\mu_0/\rho_w\mu_w$. Figure 3 plus equation (A12) can now be used to calculate the form factor H.

REFERENCES

1. Stewart, J. D., and Donaldson, C. du P.: An Analysis of Experimental Data on Transition for Blunt Bodies. Tech. Memo. 73, General Electric Co., June 24, 1957.

2. Tellep, D. M., and Hoshizaki, H.: X-17 R-9 Preliminary Flight Report - Analysis of Transition and Aerodynamic Heating. MSD 2016, Missile System Div., Lockheed Aircraft Corp., Oct. 26, 1956.

3. Wisniewski, Richard J.: Note on a Correlation of Boundary-Layer Transition Results on Highly Cooled Blunt Bodies. NASA MEMO 10-8-58E, 1958.

4. Stetson, Kenneth F.: Boundary Layer Transition on Blunt Bodies with Highly Cooled Boundary Layers. Rep. 59-36, Inst. Aero. Sci., Inc., 1959.

5. Rabb, Leonard, and Krasnican, Milan J.: Effects of Surface Roughness and Extreme Cooling on Boundary-Layer Transition for a 15° Cone-Cylinder in Free Flight at Mach Numbers to 7.6. NACA RM E57K19, 1958.

6. Dunlap, R., and Kuethe, A. M.: A Study of Instability of the Flow and Boundary Layer Transition Near the Nose of Blunt Bodies of Revolution. Pt. II: A Wind Tunnel Facility for Boundary Layer Transition Studies on a Cooled Blunt Body in Simulated Hypersonic Flow. Univ. Michigan, Sept. 1959. (Contract AF 49-638-336.)

7. Hayes, Wallace D.: On Laminar Boundary Layers with Heat Transfer. Jet Prop., vol. 26, no. 4, Apr. 1956, pp. 270-274.

8. Kemp, Nelson H., Rose, Peter H., and Detra, Ralph W.: Laminar Heat Transfer Around Blunt Bodies in Dissociated Air. Jour. Aero/Space Sci., vol. 26, no. 7, July 1959, pp. 421-430.

9. Hall, James R., Speegle, Katherine C., and Piland, Robert O.: Preliminary Results from a Free-Flight Investigation of Boundary-Layer Transition and Heat Transfer on a Highly Polished 8-Inch-Diameter Hemisphere-Cylinder at Mach Numbers up to 3 and Reynolds Number Based on a Length of 1 Foot up to 17.7×10^6. NACA RM L57D18C, 1957.

10. Seiff, Alvin, Sommer, Simon C., and Canning, Thomas N.: Some Experiments at High Supersonic Speeds on the Aerodynamic and Boundary-Layer Transition Characteristics of High-Drag Bodies of Revolution. NACA RM A56I05, 1957.

E-1007

TABLE I. - TRANSITION DATA

(a) Hemisphere

Reference	φ, deg	M_1	$Re_{d,1} \times 10^{-6}$	H_w/H_0	Re_{δ}^*	Source
1	20	11.5	20.2	0.159	-7	X-17 R-2
	30	12.0	19.6	.147	-45	X-17 R-2
	20	10.9	12.7	0.136	-31	X-17 R-8
	30	10.3	10.6	.123	-60	
	40	9.9	9.4	.115	-100	
	30	13.5	13.9	0.114	-70	X-17 R-9
	40	13.7	12.0	.091	-125	X-17 R-9
	50	12.4	23.6	0.110	-220	X-17 R-11
	60	12.4	21.9	.101	-315	X-17 R-11
	52.5	10.7	13.6	0.152	-113	X-17 R-22
	30	4.4	9.8	0.297	146	HTV RD 1
	45	4.0	9.8	.342	240	HTV RD 1
	52.5	4.0	12.0	0.407	413	HTV RD 3
	60	4.0	12.4	.383	324	HTV RD 3
	45	2.6	7.8	0.490	490	HTV RD 8
	38	2.8	24.1	0.575	838	Langley
		3.0	23.2	.544	765	
		3.1	22.2	.517	719	
9	60	3.0		0.469	574	Langley
10	40	4.0	3.80	0.241	62	Ames
4	40			0.034	-94	AVCO
	40			.057	-86	
	40			.105	-60	

(b) Blunt Cone

Reference	φ, deg	M_1	$Re_{d,1} \times 10^{-6}$	H_w/H_0	Re_{δ}^*	Source
1		7.9	20.6	0.237	352	X-17 R-17
		8.3	21.0	.245	411	
		8.7	21.5	.177	298	
		10.7	15.8	.121	123	
		11.4	23.0	0.124	114	X-17 R-18
		11.5	20.9	.114	116	
		10.0	12.4	.112	95	
		10.0	12.4	.111	100	
		13.0	7.0	0.085	30	X-17 R-21
		12.0	5.8	.077	31	X-17 R-21

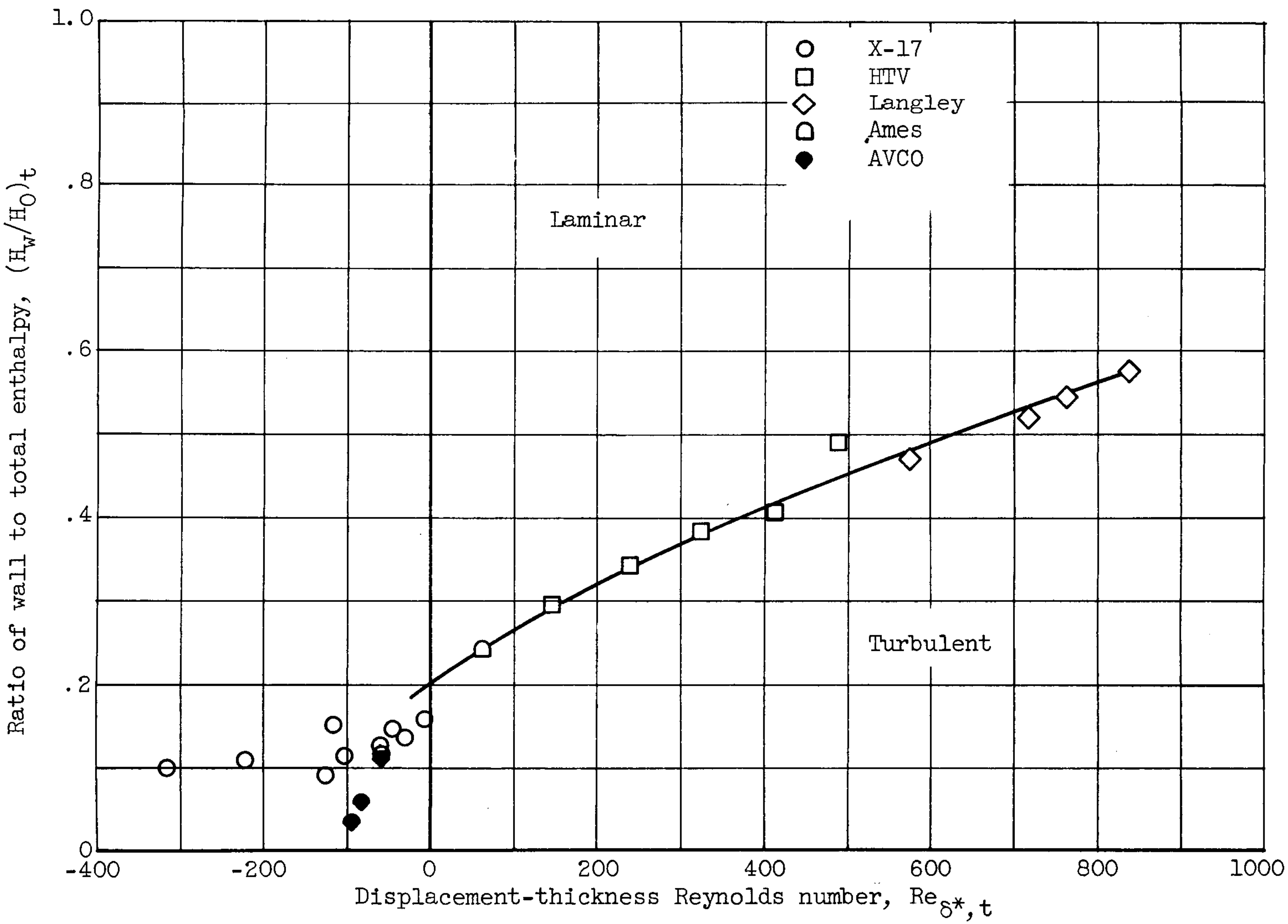

Figure 1. - Correlation of transition results on hemispheres.

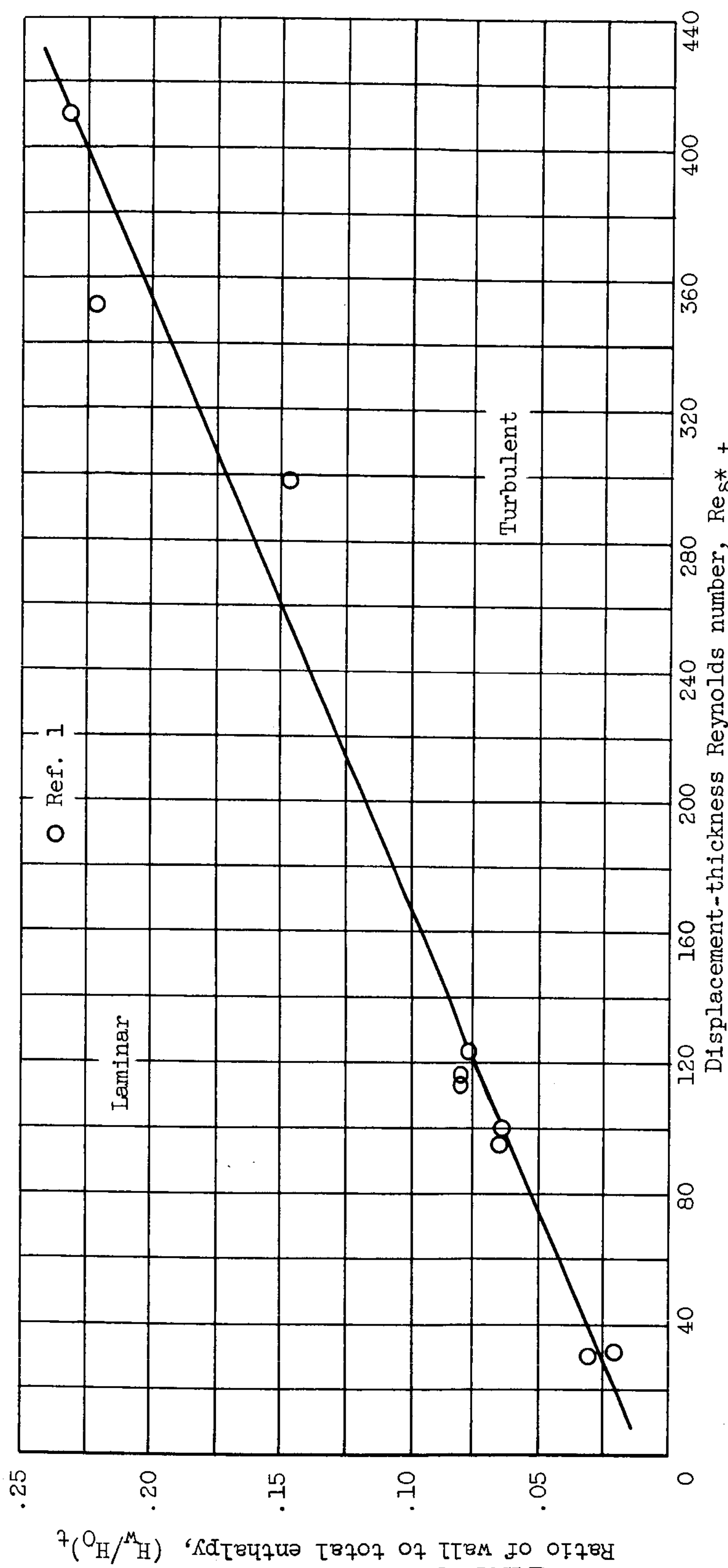

Figure 2. - Correlation of transition results on large blunt cone.

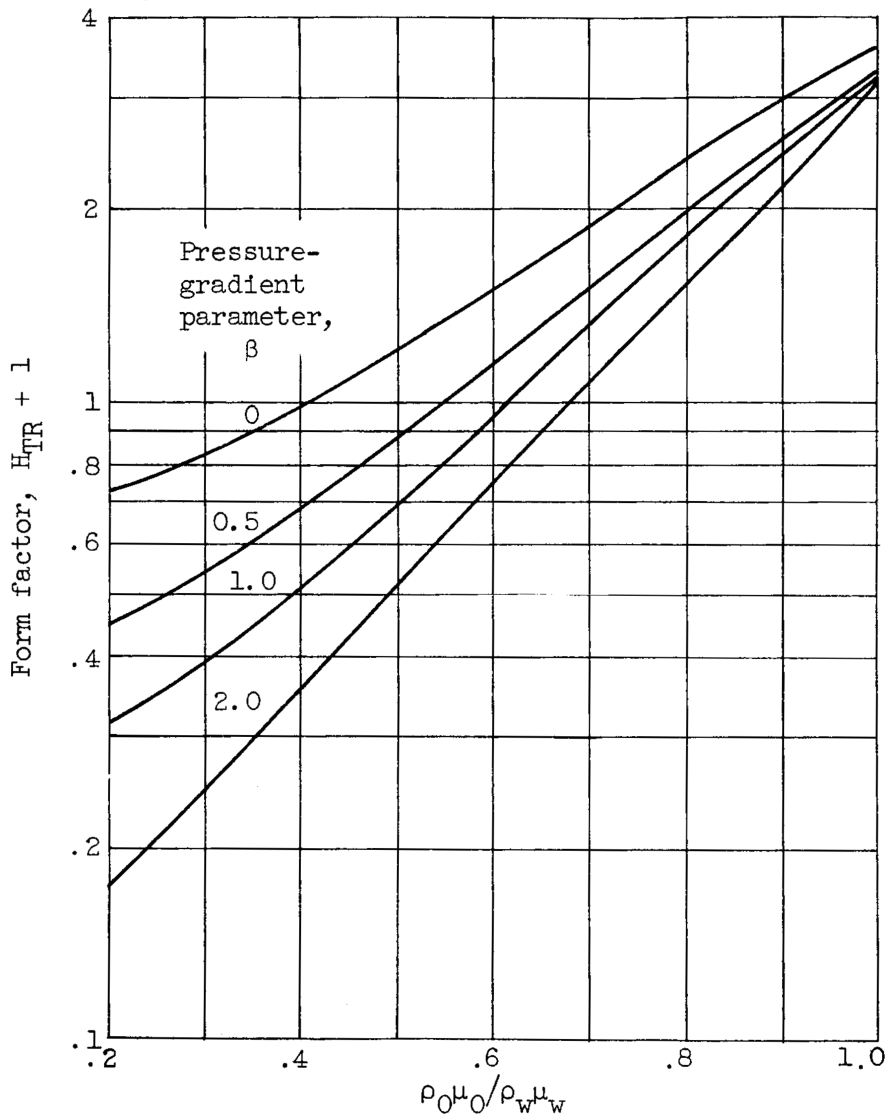

Figure 3. - Variation of transformed form factor with density-viscosity parameter.